https://doi.org/10.1016/j.apenergy.2015.09.097

TEOS/Silane Coupling Agent Composed Double Layers Structure: A Novel Super-hydrophilic Coating with Controllable Water Contact Angle Value[1]

Hu Yan[a*], Wang Yuanhao[b*] and Yang Hongxing[a]

[a] *Renewable Energy Research Group (RERG), Department of Building Services Engineering, The Hong Kong Polytechnic University, Hong Kong*

[b] *Faculty of Science and Technology, Technological and Higher Education Institute of Hong Kong, New Territories, Hong Kong*

[*] *Corresponding authors*

Abstract

The soiling of the photovoltaic (PV) modules' front surfaces decreases the power generation efficiency a lot. In this paper, a novel self-cleaning (super-hydrophilic) glass coating material with double layers' structure is prepared and the synthesis process is simple and low-price. This super-hydrophilic coating barely decreases the transparency of the glass above solar cells in the PV modules. It only reduces about 2.9% of transparency compared with original glass. Briefly, TEOS (Tetraethylorthosilicate) is skillfully utilized as hydrophobic interlayer, connected to the substrate surface and super-hydrophilic layer, whose effective component is a particular silane-coupling agent named as 2-[acetoxy (polyethyleneoxy) propyl] triethoxysilane (abbreviated as SIA). The interlayer has three advantages: firstly, after the TEOS hydrophobic layer is coated, SIA's hydrophobic siloxane terminals assemble toward this layer; Secondly, SIA's steric hindrance would decrease obviously because most of the molecules assemble orderly on the interlayer; Thirdly, TEOS provides much more grafting sites and more SIA molecules are grafted. Thus, with the increasing TEOS's concentration, the SIA's coating becomes firmer, and the SIA's concentration influences the water contact angle (CA). When it is bigger than 2.5 %, the CA is less than 10° and the surface turns to super-hydrophilic. Besides, according to the samples with different SIA's concentration and contact angle value, a fitting curve whose R^2 is higher than 0.95 is made. Based on this, the experimental contact angle value of a surface made from this SIA could be predicted. And the difference between experimental and theoretical

[1] This paper was presented at the 7th International Conference on Applied Energy (ICAE2015), March 28-31, 2015, Abu Dhabi, UAE (Original paper title: "TEOS/Silane-Coupling Agent Composed Double Layers Structure: A Novel Super-hydrophilic Surface" and Paper No.: 458).

contact angle value ranges from 1.11-5.88 %.

Keywords

Silane coupling agent; Self-cleaning; Super-hydrophilic; TEOS; Contact angle.

1. Introduction

Super-hydrophilic material has a wide application in a lot of areas such as anti-fogging [1-5], heat transfer [6-10], self-cleaning [11-13] et al. Especially in the anti-soiling of PV cells' front surfaces, since it is found that its influence on the capacity increase of PV modules is more and more obvious. The effect of dust-fouling on PV modules was studied all around the world. In Saudi Arabia, 40% degradation occurred after 6 months [14]. And in Kuwait [15], the reduction is 17%~65%, which depends on the tilt angle. The influence of dust accumulation is long-term. One effective way to solve it is cleaning the PV modules regularly. In general, the normal way is washing them by humans or some special robots. However, such ways are quite expensive since it costs a lot of water and human resources, especially when the capacity is more than 10 MW. Thus, the self-cleaning technology is applied. And it helps to enhance the efficiency of a PV cell.

Contact angle (CA) is a closely related concept with super-hydrophilic. As shown in Fig.1, when a liquid drop is on the solid surface, it is a curve due to the surface tension. And CA (θ) is the angle between the liquid-solid interface and the tangent line of the curve at the contact point of solid, liquid and gas. It could be calculated by Young's relation (1):

$$\gamma_{LV}\cos\theta = \gamma_{SV} - \gamma_{SL} \quad (1)\ [19]$$

γ_{LV}, γ_{SV}, and γ_{SL} represent the surface tension of liquid-vapor, solid-vapor, and solid-liquid respectively in equation (1). The CA represents the wettability of a solid surface, which means that the bigger the CA is, the better the wettability is, and so does the reverse. Generally speaking, it is named as hydrophobic if the CA is larger than 90°, and as hydrophilic if it is less than that. Moreover, it is called super-hydrophilic or super-hydrophobic respectively if it is less than 10° or larger than 150°. And both of the super-hydrophobic and super-hydrophilic could be considered as self-cleaning materials.

INSERT Fig. 1

The super-hydrophobic property mainly derives from the special surface structure and some coatings like polytetrafluoroethylene. [16-18] Firstly, the surface structure bases on two main super-hydrophobic theories: the Wenzel theory and Cassie-Baxter theory. [19-20] The former one mainly introduces the roughness factor into the Young's CA concept. The formula is shown below:

$$\cos\theta^{w} = r\cos\theta \quad (2)$$ [19]

In this formula, r represents the roughness factor, θ^w is the apparent CA, and θ is Young's CA. Wenzel theory reflects the state that the rough surface is fully wetted by water drop (Fig. 2a). According to Wenzel theory, for rough surface, the wettability is better than the smooth surface if it is hydrophilic originally and it is worse if the surface is hydrophobic at first. However, this theory is conflict with the fact that hydrophobic surface could be made from hydrophilic material. [21-22] Thus, Cassie and Baxter proposed the theory named after their names. The formula is shown in equation (3):

$$\cos\theta^{c} = f\cos\theta - (1-f) \quad (3)$$ [20]

In equation (3), f means solid phase fraction, θ^c is apparent CA. The wetting situation is shown in Fig. 2b that the water drop is above the stabs on the rough surface. It could be seen from equation (3), even the CA on smooth surface is quite low, a super-hydrophobic surface could be made by manipulate the surface structure which means change the value of factor f.

INSERT Fig. 2

However, in order to achieve the super-hydrophobic surface based on Cassie-Baxter model, the substrate's surface should be modified and form sophisticated nano concave-convex structure [17-22], which is very easy to be sabotaged and lose such property. In this case, super-hydrophilic material is attracting more and more attentions.

Generally, two main kinds of methods are used to achieve the super-hydrophilic surface: the organic way and inorganic way. For the organic way, hydrophilic polymers, such as PNIPAAm/PLLA (poly(N-isopropylacrylamide)/ poly(L-lactide)) [23], DMAEMA/MMA (2-(dimethylamino)-ethylmethacrylate/methyl methacrylate) [24], are always coated on the surface. However, the reaction processes is complicated including the polymerization in N_2, electrospinning and so on. And for inorganic way, the most used materials are TiO_2 [25], SiO_2

[26], In_2O_3-SnO_2 [27], Cu_2O and CuO [28]. The reaction conditions are strict too, for example the electrospinning, plasma technique and vapor deposition. Thus, in this paper, a simple way to get a super-hydrophilic coating is proposed.

The active composition, which is shown in Fig. 3, is a special silane coupling agent, named as 2-[acetoxy (polyethyleneoxy) propyl] triethoxysilane (SIA0078.0, abbreviated as SIA below). It could be seen clearly that the SIA has a long functional side chain which possesses the good hydrophilic property since there are repeated ether bonds and a carbonyl group in Fig. 3. Moreover, three -$SiOCH_2CH_3$ groups would hydrolyze into –SiOH group, and then it condensates with the –SiOH groups on the substrate surface. In this case, the SIA is grafted on the substrate and the hydrophilic side chains are toward to the outside of the substrate. Following that, the surface turns into hydrophilic. The reaction schematic picture is shown in Fig. 4.

INSERT Fig. 3

INSERT Fig. 4

However, in the practical situation, the grafting of SIA is so weak that the water could wash the coating away very easily. That is because of the existence of the long side chain in SIA molecule, the steric hindrance effect is so big that the formation of well-organized net structure is sabotaged. Thus, TEOS (molecular structure is shown in Fig. 5) is introduced in the system. As shown in Fig. 5, all of the four side chains of TEOS are –OCH_2CH_3 groups. They could be hydrolyzed into –OH groups easily. So there is no same problem for TEOS since its size is much smaller than that of SIA, thus a dense layer of TEOS would be formed even the population of silicon hydroxyl on substrate is small. Besides, the TEOS membrane brings the substrate much more –SiOH groups even though such groups are condensed as Si-O-Si groups. After that, the TEOS-pre-coated substrate reacts with SIA mentioned above, and the Si-O-Si groups of the TEOS membrane are broken and combine with the –SiOH groups which are formed after the hydrolyzation of the -$SiOCH_2CH_3$ groups in SIA. The reaction schematic picture is drawn in Fig. 6 and finally the double layers' coating is shown in Fig. 7.

INSERT Fig. 5

INSERT Fig. 6

INSERT Fig. 7

2. Experiments

The silane-coupling agent used in this paper (SIA0078.0) is purchased from the Gelest Inc (Morrisville, PA, USA). The TEOS (analytical pure) and acetic acid are from Sigma-Aldrich. The glass sheets are bought from Sail Brand Company.

In this paper, the glass sheets are used to simulate the front glass surface of PV cells. They are firstly cleaned by detergent and clean water. After dried in room temperature, those sheets are soaked in TEOS solutions with different concentration. When dried, they are merged into SIA solution (with different concentration and adjust the pH around 5.5 with acetate acid). The system is heated to 75℃ for 10 minutes.

The UV-vis spectra are gathered from Lambda 750, PerkinElmer. The FT-IR data are obtained by Nicolet iS50 FT-IR, Thermo Scientific. Contact Angle Goniometer Sindatek Model 100SB is used to measure the contact angle.

3. Results and discussions

3.1. The comparison of TEOS/SIA double layers' coating and SIA single layer coating

The SIA's single layer coating provides the surface very good hydrophilic property. However, the coating firmness is so weak that the hydrophilic property is very easy to lose. With the help of TEOS, the SIA could be coated much more firmly. In this part, the comparison is made by making samples with TEOS/SIA coating and SIA single layer coating.

For the TEOS/SIA coating sample, the substrate is firstly coated with pure TEOS by pulling method (the speed is 0.3cm/s and for 3 times), then it is soaked in the SIA solution (2.4%, pH 5.5) for 10min at the temperature of 75℃. And for the SIA coating sample, the glass sheet is directly soaked in the same SIA solution. After soaked in DI water for 12h, their CA values are measured and compared, which is shown in Fig. 8. Fig. 9 shows the FT-IR curves of those two samples.

INSERT Fig. 8

INSERT Fig. 9

It could be seen clearly that TEOS contributes a lot to the firmness of the SIA coating. After the soaking process, the hydrophilicity of SIA coating sample disappeared while the TEOS/SIA coating still possesses the super-hydrophilicity. The probable reason is in SIA single layer coating, the SIA is absorbed on the surface or grafted on the surface by very weak bonds like Van der Waals' force or hydrogen bond since there are no sufficient sites for the SIA's grafting on the surface. Moreover, In this case, the coating is so weak that the super-hydrophilicity would disappear easily. And moreover, from the "TEOS/SIA curve" in Fig. 9, the peaks at 2975 and 2885 cm^{-1} are the stretching vibration peaks of the $-CH_3$ groups in the sample, and the peak at 1736 cm^{-1} represents the C=O bond, the peak at 1136 cm^{-1} is the C-O stretching vibration peak. Those characteristic peaks represent the groups in the SIA. Thus it is demonstrated that the SIA molecules are grafted on the surface. Compared with it, the "SIA" curve barely has detectable infrared absorption peak, which means there are almost no SIA molecule on the surface. Given the information of CA and FT-IR curve, conclusion could be made that TEOS contributes a lot to the firmness of SIA's grafting.

3.2. The transparency of the double-layer coating glass

For the application in the PV area, the transparency, especially in visible light band (390~700nm), is an important property. Thus, the UV-Vis tests are made. The comparison between the original glass and the double-layer coated glass mentioned above is shown in Fig. 10. And since the original y-axes in UV-Vis spectrum is absorbance, which is a logarithmic unit. It is inconvenient to compare the transparency. Thus it is transferred into transmittance.

INSERT Fig. 10

As shown in Fig. 10, the two curves barely have differences. It only occurs in the wave band from 400~650nm. And the transmittance reduction ranges from 0% to less than 2.9%. The reduction is decreasing with the increase of the wavelength. This figure demonstrates that the coating has no obvious influence on the transmittance.

3.3. The influence of SIA concentration

In this section, the influence of SIA's concentration on the hydrophilic property is studied. The substrates are pre-coated with pure TEOS and then react with those SIA solutions with different concentrations. In order to detect the firmness of the SIA coating, the

CA values of such samples before and after soaked in DI water are measured. The CA values are shown in Table. 1. The curves for the CA values are shown in Fig. 11.

INSERT TABLE 1

INSERT Fig. 11

From the data above, it could be seen clearly that after those samples are soaked in DI water for 12h, the super-hydrophilicity still remains. And from Fig. 11, after the SIA concentration is bigger than 0.8%, the CA has a huge decrease, which changes from 83° to 20.45°. This is probably because only when the concentration is more than 0.8% are there sufficient SIA molecules grafted on the TEOS layer. And when the concentration is bigger than that, with the gradually increase, the CA is decreasing slowly too. After it reaches 2.5%, the CA is below 10 degree and the surface turns to be super-hydrophilic. Besides that, two power function fitting curves are drawn for "CA before soaked in water" and "CA after soaked in water". The formulas are shown below:

$$y = 16.8685x^{-0.68954} \tag{4}$$

$$y = 17.40437x^{-0.67729} \tag{5}$$

Equation (4) is the fitting for the "CA before soaked in water" and equation (5) is for the "CA after soaked in water". Among them, y represents the value of contact angle and x is for the concentration of SIA. Those two fitting curves both have relatively high R^2, which are 0.95035 and 0.95494. Thus it is possible to predict the contact angle according to SIA's concentration. Or even reversely, by controlling the concentration, it is possible to produce a surface with specific contact angle value.

Additionally, as shown in Fig. 11, the contact angle value barely changes when it is before or after soaked in water. It means that with the help of TEOS as the interlayer, the firmness of SIA is improved. Thus, in order to study the influence of TEOS's concentration on the double layer coating, the concentration of SIA is set as 2.5% when the TEOS's concentration varies from 15% to 100%.

3.4. The influence of TEOS concentration

Like the section 3.2, the CA values, which are before and after soaked in DI water for 12h, of different samples, made by different TEOS concentrations, are measured respectively.

They are shown in Table. 2. The CA curves depending on the TEOS concentration is shown in Fig. 12.

INSERT TABLE 2

INSERT Fig. 12

From Fig. 12, conclusion could be made that with the increase of TEOS concentration, the CA values before soaked in water approach the values after soaked in water gradually. In another word, the grafting of SIA on the TEOS layer becomes firmer and firmer. And starting from the concentration of 45%, the firmness of the SIA's grafting has a huge increase. It is probably because when the TEOS's concentration reaches this value, a relatively dense TEOS layer forms and then it provides enough grafting sites for SIA. While from the 15% to 45%, it has a huge gap between the two curves in Fig. 12, the probably reason is TEOS with those concentrations may not form a dense layer which has enough graft sites for the SIA condensing into a crosslinking net (Fig. 13.a) but an isolated structure (Fig. 13.b). Before such samples are soaked in water, in the area, which has no TEOS layer, SIA is absorbed on the substrate by very weak bond, such as Van der Waals' force or hydrogen bond, so the super-hydrophilicity still works. But once they are soaked in water, such SIA molecules with weak cross-linking will be washed away from the substrate. And when TEOS concentration is beyond 90%, such crosslinking structure in Fig. 13.a is formed. Then, the firmness would be enhanced.

INSERT Fig. 13

3.5. The synthesis of a coating with specific contact angle

As shown in section 4.2, equation (4) and equation (5) describe the possible value relation between the value of contact angle and SIA's concentration. And the fitting curves' relativity is commendable. Therefore it is possible to predict the contact angle according to the SIA's concentration or do the converse.

Three samples with different concentrations of SIA are made to test the equation (4). The theoretical and experimental values are shown in Table. 3 and the contact angle pictures are shown in Fig. 14.

INSERT TABLE 3

INSERT Fig. 14

As shown in Table 3 and Fig 14, even though the difference percentage ranges from 1.11-5.88 %, equation (4) could predict the relation between SIA's concentration and the contact value to a great extent. Certainly, this formula has the limitation that it is only based on those specific reaction materials and method. However, it provides a way to synthesis a coating with particular contact angle. And with more accurate reaction condition and more samples the relation could be more precise.

4. Conclusions

From the results above, conclusion could be drawn that the TEOS/SIA double layer structure does enhance the firmness of SIA's grafting on the substrate a lot. Since the much smaller steric hindrance effect because of the small size of TEOS compared with that of SIA, the pre-coating of TEOS forms a dense layer structure, which provides much more silicon hydroxyls for the grafting of SIA. At last, the firmness of SIA's coating is enhanced.

And the concentration of TEOS influences the firmness of SIA's coating while the SIA's concentration affects the super-hydrophilicity. When the TEOS's concentration is larger than 45%, the enhancement of SIA's grafting is obvious, and the more the TEOS is, the firmer the coating would be. If the concentration is 100%, the firmness is the best. And for SIA's concentration, the bigger it is, the smaller the CA would be. After the concentration approaches 0.8%, the effect of the increase of concentration is not obvious.

Additionally, by analyzing the SIA's concentrations and contact angle values of 28 samples, a formula with high relativity is fitted. According to this formula, new-made samples' experimental values and theoretical values are contrasted. The results show the difference percentage ranges from 1.11-5.88 %. And if with much more accurate reaction conditions and more samples, the formula will be more precise.

The method in this work provides a very simple way to produce a super-hydrophilic surface. And its low cost suits the cost sensible area like PV cells. But, besides the PV cells filed, the coating would be used in anti-fogging, curtain wall self-cleaning, etc.

Acknowledgements

The work described in this paper was supported by a grant from the CII-HK / PolyU

Innovation Fund. Great help from Department of Applied Biology & Chemical Technology and Research Institute for Sustainable Urban Development (RISUD) of The Hong Kong Polytechnic University is appreciated.

References

[1] Tricoli A, Righettoni M, Pratsinis S E. Anti-Fogging Nanofibrous SiO_2 and Nanostructured SiO_2-TiO_2 Films Made by Rapid Flame Deposition and In Situ Annealing[J]. Langmuir, 2009, 25(21): 12578-12584.

[2] Jia Y, Liu G, Wu X, et al. Anti-fogging and anti-reflective silica nanofibrous film fabricated by seedless flame method[J]. Materials Letters, 2013, 108: 200-203.

[3] Han Y C, Lee S, Ahn B H, et al. Preparation of anti-fogging low density polyethylene film by using γ-irradiation[J]. Sensors and Actuators B: Chemical, 2007, 126(1): 266-270.

[4] Chen Y, Zhang Y, Shi L, et al. Transparent superhydrophobic/ superhydrophilic coatings for self-cleaning and anti-fogging[J]. Applied Physics Letters, 2012, 101(3): 033701.

[5] Park J T, Kim J H, Lee D. Excellent anti-fogging dye-sensitized solar cells based on superhydrophilic nanoparticle coatings[J]. Nanoscale, 2014, 6(13): 7362-7368.

[6] Yamada Y, Ikuta T, Nishiyama T, et al. Droplet Nucleation on a Well-Defined Hydrophilic–Hydrophobic Surface of 10-nm Order Resolution[J]. Langmuir, 2014.

[7] Jo H J, Ahn H S, Kang S H, et al. A study of nucleate boiling heat transfer on hydrophilic, hydrophobic and heterogeneous wetting surfaces[J]. International Journal of Heat and Mass Transfer, 2011, 54(25): 5643-5652.

[8] Macner A M, Daniel S, Steen P H. Condensation on Surface Energy Gradient Shifts Drop Size Distribution toward Small Drops[J]. Langmuir, 2014, 30(7): 1788-1798.

[9] Hagiwara I, Tokuhiro A, Oduor P G. Natural convection heat transfer of hydrophilic particle suspension: Implications on nuclear waste remediation[J]. International Journal of Heat and Mass Transfer, 2014, 78: 636-647.

[10] Hao T, Ma X, Lan Z, et al. Effects of hydrophilic surface on heat transfer performance and oscillating motion for an oscillating heat pipe[J]. International Journal of Heat and Mass Transfer, 2014, 72: 50-65.

[11] Kim S, Cheung E, Sitti M. Wet self-cleaning of biologically inspired elastomer mushroom shaped microfibrillar adhesives[J]. Langmuir, 2009, 25(13): 7196-7199.

[12] Caschera D, Cortese B, Mezzi A, et al. Ultra hydrophobic/superhydrophilic modified cotton textiles through functionalized diamond-like carbon coatings for self-cleaning applications[J]. Langmuir, 2013, 29(8): 2775-2783.

[13] Diamanti M V, Gadelrab K R, Pedeferri M P, et al. Nanoscale investigation of photoinduced hydrophilicity variations in anatase and rutile nanopowders[J]. Langmuir, 2013, 29(47): 14512-14518.

[14] Nimmo B, Said SAM. Effects of dust on the performance of thermal and photovoltaic flat plate collectors in Saudi Arabia—preliminary results. In: Veziroglu TN, editor. Proceedings of the 2nd Miami International Conference on Alternative Energy Sources, Dec. 10–13. 1979. p. 223–5.

[15] Sayigh A, Al-Jandal S, Ahmed H. Dust effect on solar flat surfaces devices in Kuwait. In:

Furlan C, Mancini NA, Sayigh AAM, Seraphin BO, editors. Proceedings of the Workshop on the Physics of Non-Conventional Energy Sources and Materials Science for Energy, 1985 Sept. 2–20. 1985. p. 353-367.

[16] Zhao X, Chen W, Su Y, et al. Hierarchically engineered membrane surfaces with superior antifouling and self-cleaning properties[J]. Journal of membrane science, 2013, 441: 93-101.

[17] Weng K W, Huang Y P. Preparation of TiO_2 thin films on glass surfaces with self-cleaning characteristics for solar concentrators[J]. Surface and Coatings Technology, 2013, 231: 201-204.

[18] Feng L, Li S, Li Y, et al. Super-hydrophobic surfaces: from natural to artificial[J]. Advanced materials, 2002, 14(24): 1857-1860.

[19] Wenzel R N. Resistance of solid surfaces to wetting by water[J]. Industrial & Engineering Chemistry, 1936, 28(8): 988-994.

[20] Cassie A B D, Baxter S. Wettability of porous surfaces[J]. Transactions of the Faraday Society, 1944, 40: 546-551.

[21] Cao L, Hu H H, Gao D. Design and fabrication of micro-textures for inducing a superhydrophobic behavior on hydrophilic materials[J]. Langmuir, 2007, 23(8): 4310-4314.

[22] Anish Tuteja, Wonjae Choi, Minglin Ma, et al. Designing superoleophobic surfaces[J]. Science, 2007, 318, 1618-1622.

[23] Gu S Y, Wang Z M, Li J B, et al. Switchable Wettability of Thermo‐Responsive Biocompatible Nanofibrous Films Created by Electrospinning[J]. Macromolecular Materials and Engineering, 2010, 295(1): 32-36.

[24] Zhao J, Meyer A, Ma L, et al. Acrylic coatings with surprising antifogging and frost-resisting properties[J]. Chemical Communications, 2013, 49(100): 11764-11766.

[25] Wang R, Hashimoto K, Fujishima A, et al. Light-induced amphiphilic surfaces[J]. Nature, 1997, 388: 431-432.

[26] Machida M, Norimoto K, Watanabe T, et al. The effect of SiO2 addition in super-hydrophilic property of TiO2 photocatalyst[J]. Journal of Materials science, 1999, 34(11): 2569-2574.

[27] Premkumar J R, Khoo S B. Electrochemically generated super-hydrophilic surfaces[J]. Chemical communications, 2005 (5): 640-642.

[28] Tang K, Wang X, Yan W, et al. Fabrication of superhydrophilic Cu_2O and CuO membranes[J]. Journal of membrane science, 2006, 286(1): 279-284.

FIG. CAPTIONS

Fig. 1 Contact angle θ; γ LV: liquid-vapor surface tension; γSV: solid-vapor surface tension; γSL: solid-liquid surface tension

Fig. 2 The wetting situation of super-hydrophobic. a: Wenzel situation; b: Cassie-Baxter situation

Fig. 3 The molecular structure of SIA0078.0

Fig. 4 The reaction between SIA and substrate; R represents the hydrophilic side chain in SIA

Fig. 5 The molecular structure of TEOS

Fig. 6 The schematic picture of the reaction between SIA and TEOS-pre-coated substrate

Fig. 7 The diagram of the double layers' coating; TEOS;  SIA

Fig. 8 The CA values after soaked in DI water for 12h; a: SIA single layer coating; b: TEOS/SIA double layers' coating

Fig. 9 The FT-IR spectrum of samples soaked in DI water; SIA: the sample of SIA single layer coating; TEOS/SIA: the sample of TEOS/SIA double layers coating

Fig. 10 The comparison of transmittance between the original glass and coated glass

Fig. 11 The contact angle based on the SIA concentration

Fig. 12 The contact angle based on the TEOS concentration

Fig. 13 a. the double layer structure with sufficient TEOS concentration; b. the double layer structure with insufficient TEOS concentration

Fig. 14 The experimental contact angle from sample H to L

Figure

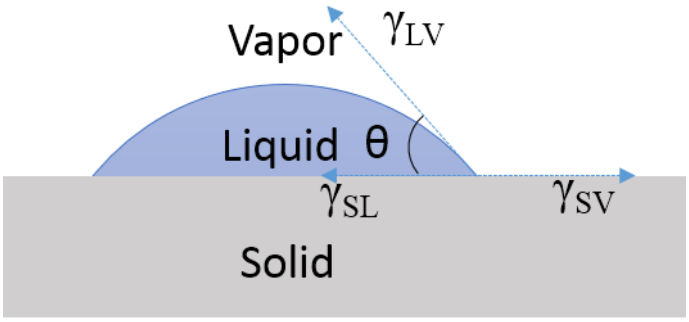

Fig. 1. Contact angle θ

γ_{LV}: liquid-vapor surface tension; γ_{SV}: solid-vapor surface tension; γ_{SL}: solid-liquid surface tension

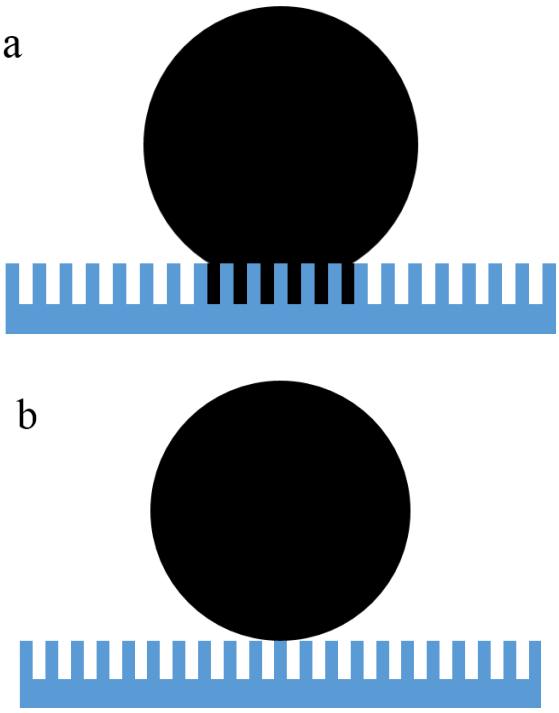

Fig. 2. The wetting situation of super-hydrophobic.

a: Wenzel situation; b: Cassie-Baxter situation

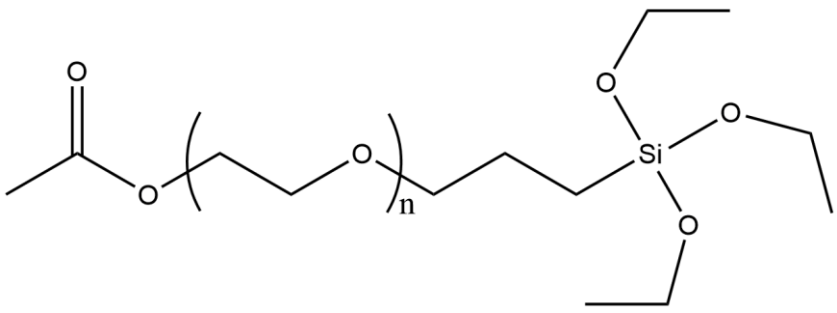

Fig. 3. The molecular structure of SIA0078.0

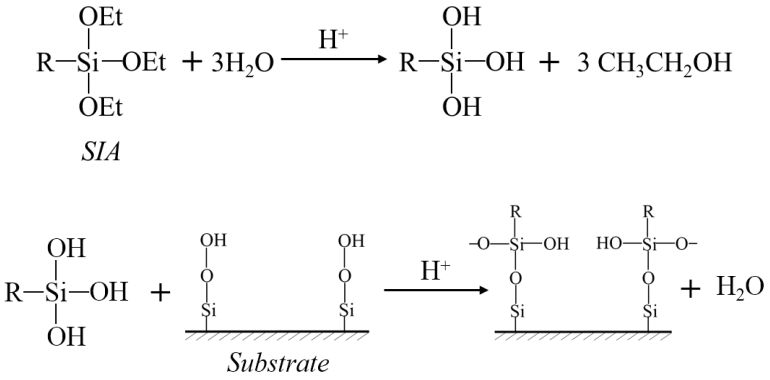

Fig. 4. The reaction between SIA and substrate

R represents the hydrophilic side chain in SIA

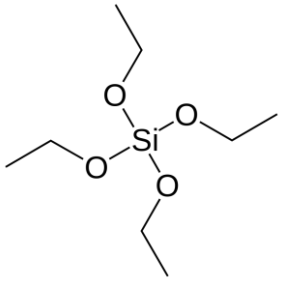

Fig. 5. The molecular structure of TEOS

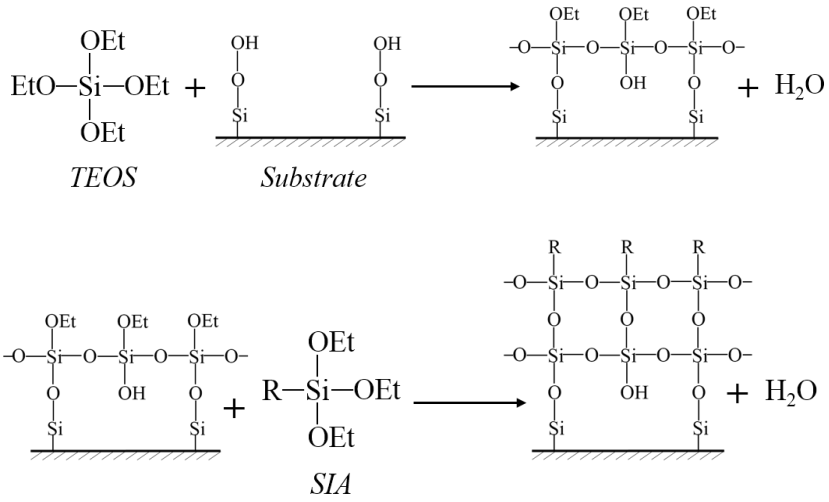

Fig. 6. The schematic picture of the reaction between SIA and TEOS-pre-coated substrate

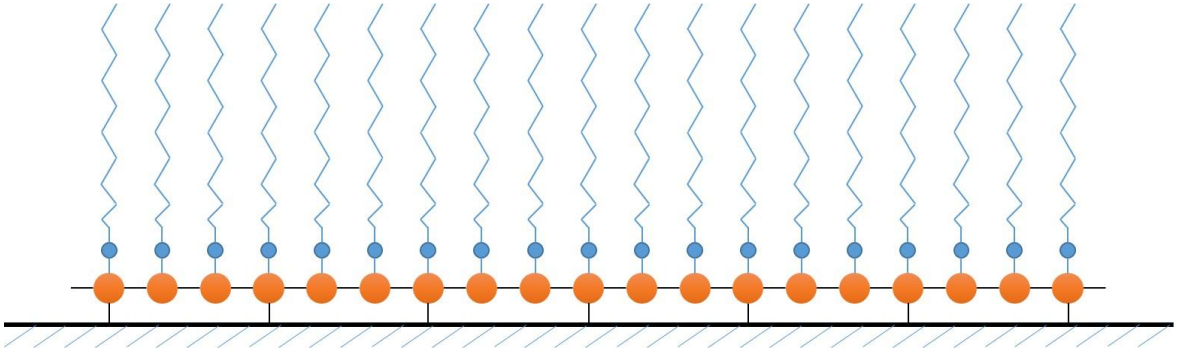

Fig. 7. The diagram of the double layers' coating

TEOS

SIA

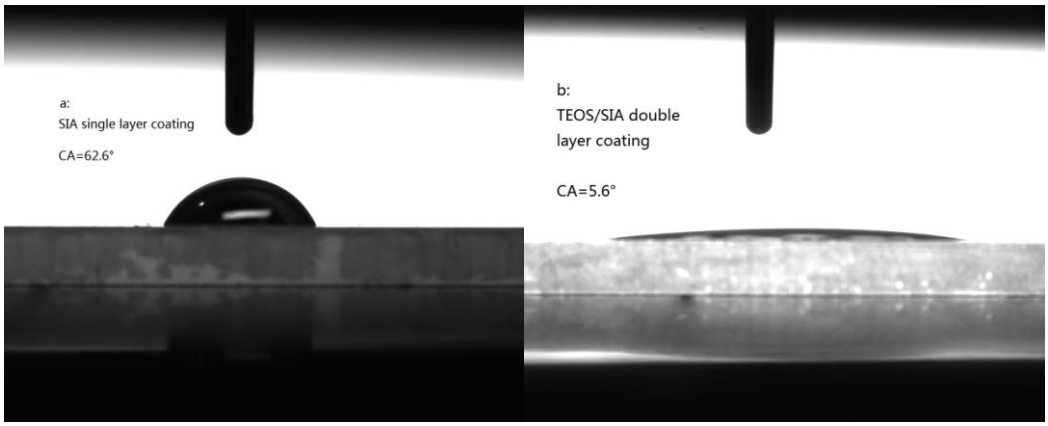

Fig. 8. The CA values after soaked in DI water for 12h

a: SIA single layer coating; b: TEOS/SIA double layers' coating

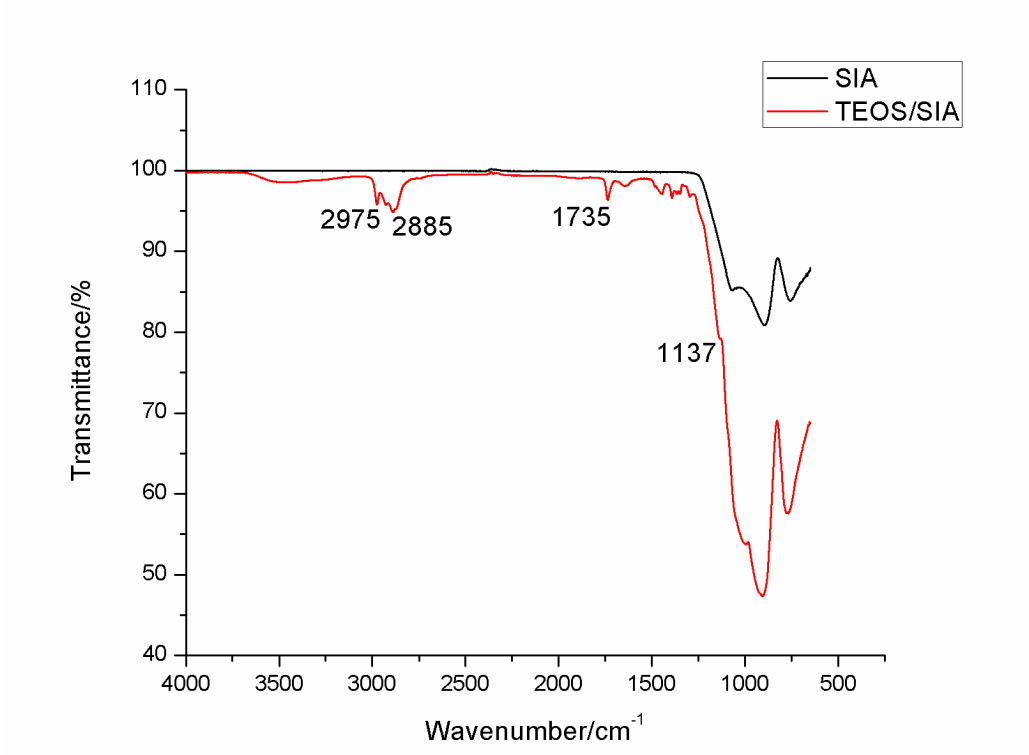

Fig. 9. The FT-IR spectrum of samples soaked in DI water

SIA: the sample of SIA single layer coating

TEOS/SIA: the sample of TEOS/SIA double layers coating

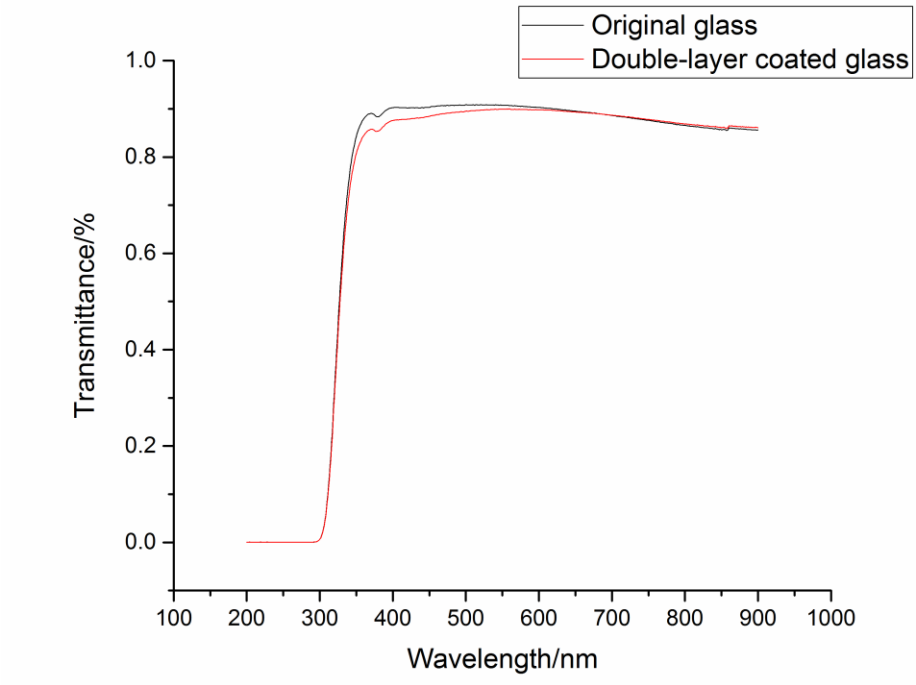

Fig. 10. The comparison of transmittance between the original glass and coated glass

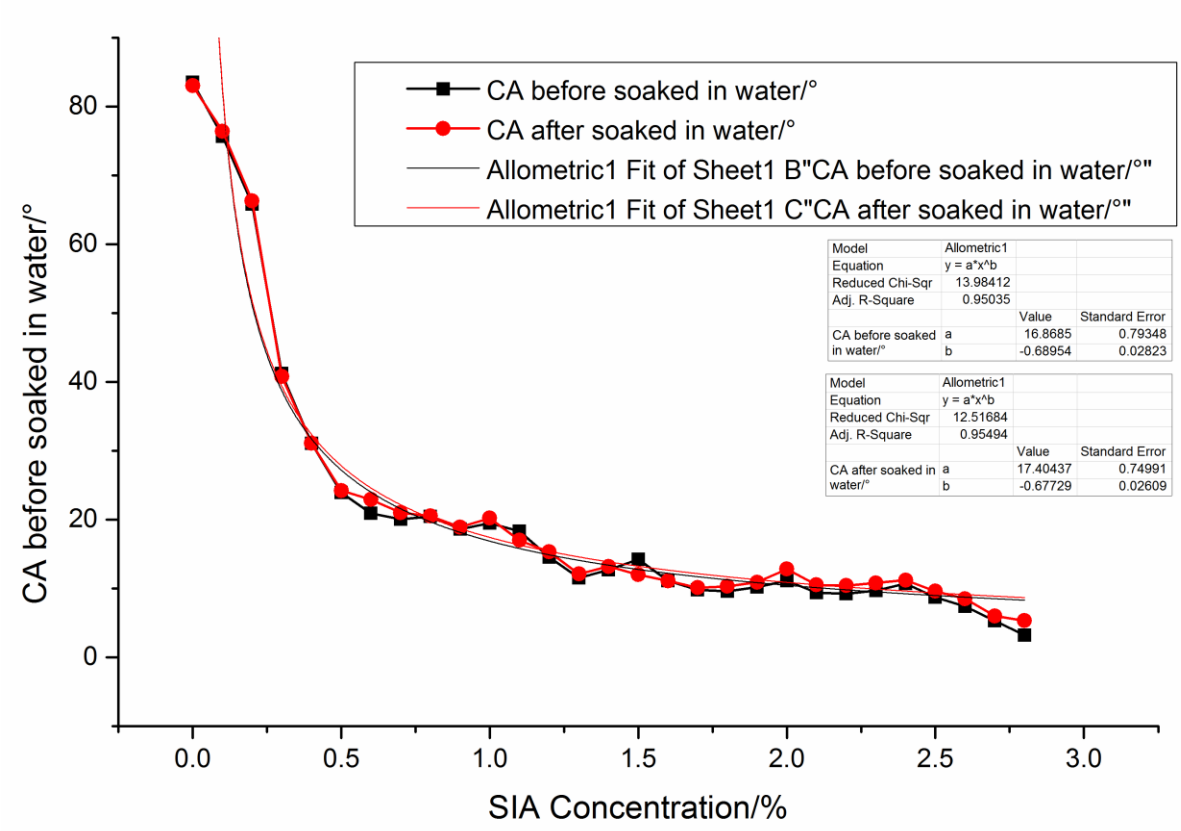

Fig. 11. The contact angle based on the SIA concentration

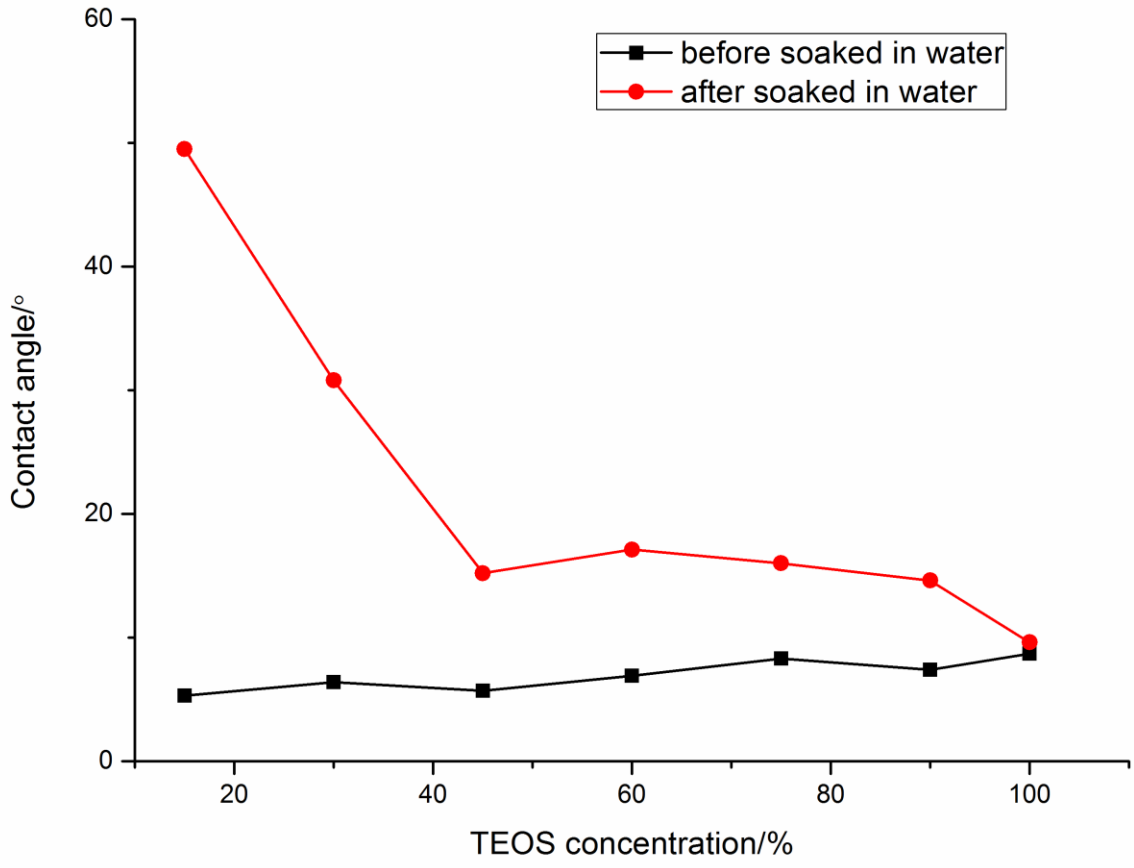

Fig. 12. The contact angle based on the TEOS concentration

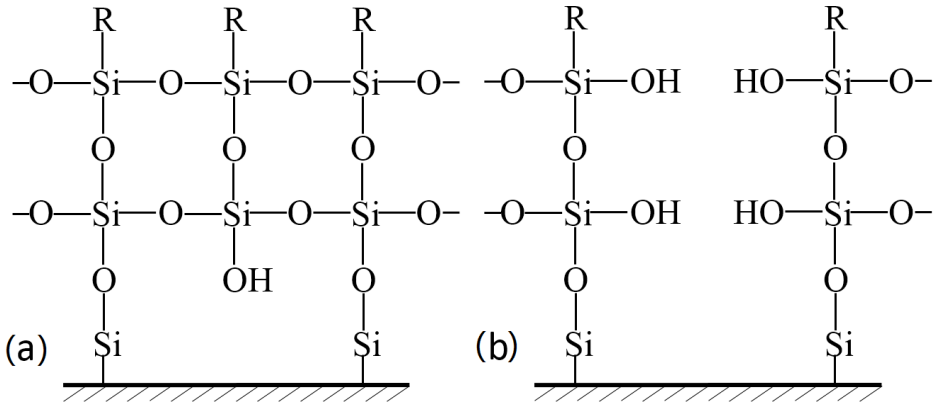

Fig. 13. a. the double layer structure with sufficient TEOS concentration

b. the double layer structure with insufficient TEOS concentration

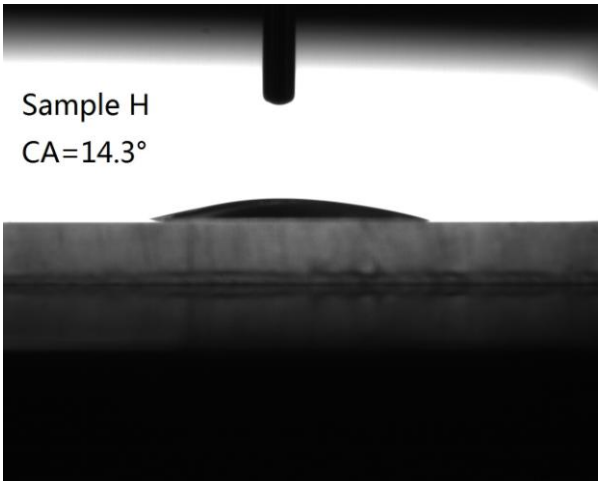
Sample H
CA=14.3°

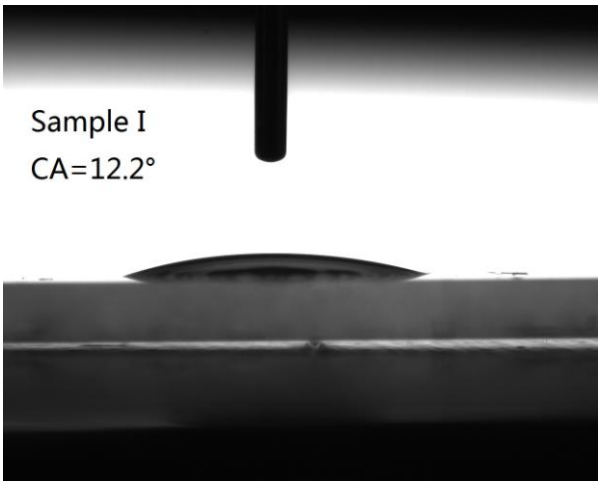
Sample I
CA=12.2°

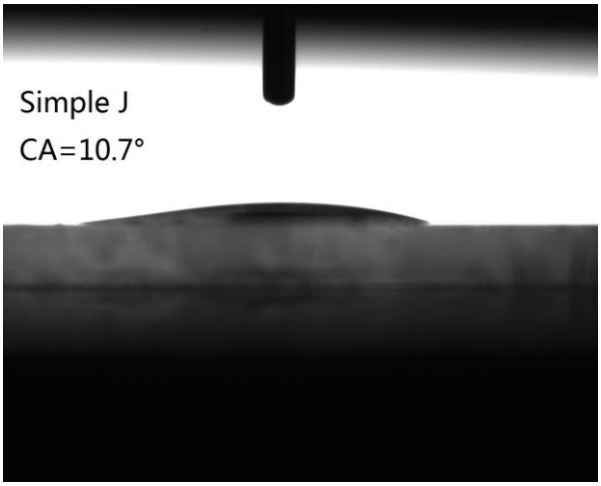
Simple J
CA=10.7°

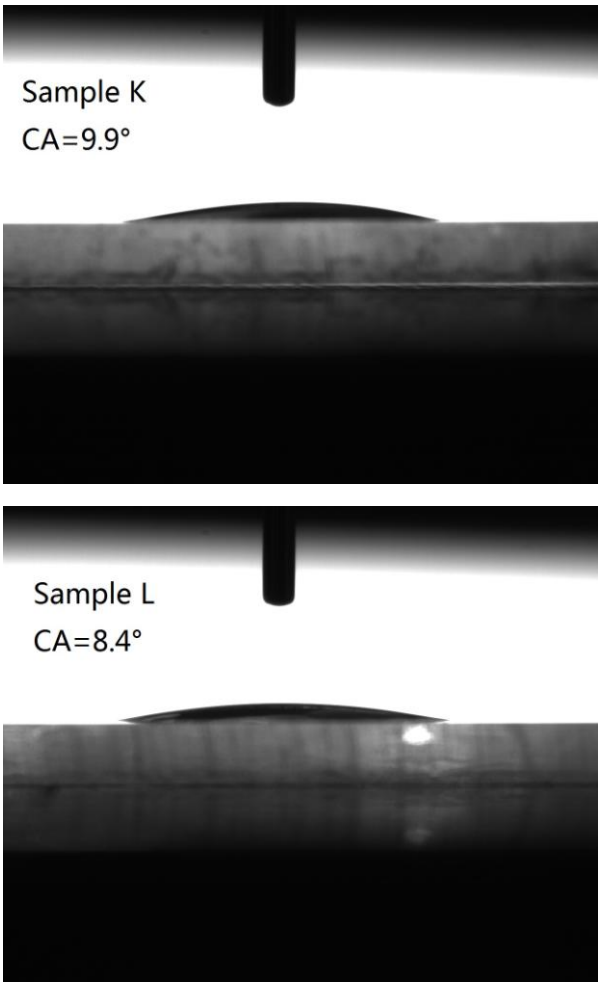

Fig. 14. The experimental contact angle from sample H to L

Table

Table. 1. The CA values depends on different SIA concentration

Samples	SIA Concentrations/%	CA before soaked in water/°	CA after soaked in water/°
1	0	83.5	830.
2	0.1	75.66	76.4
3	0.2	65.8	66.3
4	0.3	41.21	40.8
5	0.4	31.04	31.06
6	0.5	23.9	24.2
7	0.6	20.9	22.9
8	0.7	20.04	21.0
9	0.8	20.45	20.5
10	0.9	18.6	18.9
11	1.0	19.5	20.2
12	1.1	18.3	17.0
13	1.2	14.52	15.3
14	1.3	11.5	12.1
15	1.4	12.7	13.2
16	1.5	14.2	12.0
17	1.6	11.1	11.1
18	1.7	9.8	10.1
19	1.8	9.6	10.3
20	1.9	10.2	10.9
21	2	11.1	12.8
22	2.1	9.4	10.5
23	2.2	9.2	10.4
24	2.3	9.7	10.8
25	2.4	10.7	11.2
26	2.5	8.7	9.6
27	2.6	7.4	8.5
28	2.7	5.3	6.0
29	2.8	3.2	5.3

Table. 2. The CA values depends on different TEOS concentrations

Samples	A	B	C	D	E	F	G
TEOS concentrations/%	15	30	45	60	75	90	100
CA before soaked in water/°	5.3	6.4	5.7	6.9	8.3	7.4	8.7
CA after soaked in water/°	49.5	30.8	15.2	17.1	16	14.6	9.6

Table. 3. The theoretical and experimental contact angle values

Samples	H	I	J	K	L
SIA concentrations/%	1.25	1.55	1.85	2.35	2.85
Theoretical CA values before soaked in water/°	14.46	12.47	11.04	9.35	8.19
Experimental CA values before soaked in water/°	14.3	12.2	10.7	9.9	8.4
Difference percentages/%	1.11	2.16	3.08	5.88	2.56